Minimal requirements for membrane adaptation of the bacterial model organism *M. extorquens*

Grzegorz Chwastek [1], Michal A. Surma [2,3,] ORCID, Sandra Rizk [1,] ORCID, Daniel Grosser [4], Oksana Lavrynenko [5], Magdalena Rucińska [1], Helena Jambor [6,] ORCID, James Sáenz [1,*,] ORCID

1 Technische Universität Dresden, B CUBE, Tatzberg 41, Dresden, DE

2 Lipotype GmbH, Tatzberg 47, Dresden, DE

3 Łukasiewicz Research Network – PORT Polish Center for Technology Development, Stabłowicka 147, Wrocław, PL

4 DZD-Paul Langerhans Institute Dresden, Fetscherstraße 74, Dresden, DE

5 Max Planck Institute of Molecular Cell Biology and Genetics, Pfotenhauerstraße 108, Dresden, DE

6 Technische Universität Dresden, Medizinische Fakultät, Fetscherstraße 74, Dresden, DE

* corresponding author and lead contact: james.saenz@tu-dresden.de

Keywords: Lipidomics, Membrane organization, Adaptation, Lipidome resource

Abstract

Cells, from microbes to man, adapt their membranes in response to the environment to maintain functionality. How cells sense environmental change/stimuli and adapt their membrane accordingly is unclear. In particular, how lipid composition changes and what lipid structural features are necessary for homeostatic adaptation remains relatively undefined. Here, we examine the simple yet adaptive lipidome of the plant-associated Gram-negative bacterium *Methylobacterium extorquens* over a range of chemical and physical conditions. Using shotgun lipidomics, we explored adaptivity over varying temperature, hyperosmotic and detergent stress, carbon sources, and cell density. Globally, we observed that as few as 10 lipids, representing ca. 30% of the lipidome, characterized by 9 structural features account for 90% of the total changes. We revealed that variations in lipid structural features are not monotonic over a given range of conditions (e.g. temperature) and are not evenly distributed across lipid classes. Thus, despite the compositional simplicity of this lipidome, the patterns in lipidomic remodeling suggest a highly adaptive mechanism with many degrees of freedom. Our observations reveal constraints on the minimal lipidomic requirements for an adaptive membrane and provide a resource for unraveling the design principles of living membranes.

1. Introduction

All organisms have at least one membrane that is crucial for compartmentalizing and coordinating biochemical processes within the cell. And yet, nearly a century since the discovery that membranes are made of a lipid bilayer (Gorter and Grendel, 1925) and half a century since integral membrane proteins were proposed in the Fluid Mosaic model (Singer and Nicolson, 1972) we still lack fundamental insight into the design principles required to engineer a functional cell membrane. Much of the membrane's functionality is associated with the activity of membrane proteins, which perform a diverse range of tasks from signaling to transport. The activity of such proteins is in turn crucially dependent on the biophysical properties of the membrane such as viscosity, thickness, curvature and bilayer asymmetry (Hunte and Richers, 2008; Klose et al., 2013; Pomorski and Menon, 2006; Sanders and Mittendorf, 2011). These properties are largely dictated by membrane lipids (Ernst et al., 2016; van Meer et al., 2008).

Cells produce many lipids with different structures that, in their unique combinations, determine the membrane's biophysical state. Moreover, cellular lipidomes can vary from tens, for example in the bacterial lipidome reported here, to hundreds of individual lipid species in mammalian cells (Sampaio et al., 2011; van Meer et al., 2008). A major challenge in membrane research is, therefore, to understand how cells regulate individual lipid abundances to maintain an adaptive, functional membrane. Recent progress reconstituting synthetic membranes from the bottom up is paving the way towards the goal of building a self-sustaining adaptive membrane and presently one of the challenges is to implement adaptive lipid remodeling (Brea et al., 2016; Buddingh and van Hest, 2017; Hardy et al., 2015; Tang et al., 2014). Complex lipidomes can be remodeled to modulate collective membrane properties such as viscosity, lipid packing, thickness and phase properties (Klose et al., 2013; Levental et al., 2016). For instance, increasing the proportion of lipids containing double bonds (acyl chain saturation) or changing the number or position of double bonds along the phospholipid acyl chains, can alter the overall membrane viscosity (Quinn, 1981).

Singular observations of lipidome composition do not inform which properties the cell membrane senses and adapts to, nor which minimal suite of lipid structure are required for swift adaptation. Lipidomics has provided global insights into the complexity of cellular lipidomes from yeast to man and can provide insight into how cells remodel lipid composition during adaptation (Ejsing et al., 2009). To date, however, there still are only few studies systematically characterizing lipidomic remodeling across a range of conditions and stressors. The most comprehensive study of this kind

66 was performed on yeast (Klose et al., 2012), whose lipidome contains over 150 unique lipids,
67 providing unprecedented insight into the adaptation of a complex eukaryotic lipidome.
68
69 Complex organisms possess membranes with diverse and niche-specific functional requirements.
70 While understanding complex lipidomes is important, such systems are not ideal for exploring the
71 fundamental principles underlying lipidome adaptation. Since all membranes require means to
72 homeostatically adapt to perturbations (Kaiser et al., 2011), a simpler organism that is capable of
73 adapting to a broad range of environmental conditions would be a more suitable model system to
74 elucidate the minimal lipidomic requirements for adaptation. Bacteria are an attractive target for this
75 endeavor since some are among the simplest organisms, capable of surviving over a broad range of
76 environments, and many species have been well-characterized and established as model organisms
77 for cell biology.
78
79 Here, we characterized the lipidomic adaptivity of the Gram-negative bacterium *Methylobacterium*
80 *extorquens*. *M. extorquens* has a small lipidome, with 25 phospholipid species as compared with over
81 100 in *E. coli* (Jeucken et al., 2019). Despite its relatively small lipidome, as a plant- and soil-
82 associated bacterium, *M. extorquens* must adapt to a broad range of chemical and physical conditions
83 (Vorholt, 2012). We explored the lipidome variation over varying temperature, osmotic and detergent
84 stress, carbon source, and cell density. Surprisingly, we find that most lipidome features remain
85 stable, with only minimal modulations even under significant perturbations. However, other lipidome
86 features are highly plastic and contribute to membrane adaptation. Analysis of structural features such
87 as saturation, acyl chain length or headgroup type revealed signatures of adaptive lipidomes.
88 Globally, we observed that as few as 10 lipids, less than 30% of all available species, account for the
89 majority of lipidomic adaptation across all perturbations. The patterns of lipidome remodeling that
90 we report here provide a resource for exploring the minimal design principles of living membranes
91 and for designing an adaptive synthetic membrane.
92
93 **2. Results and Discussion**
94
95 **2.1 Experimental Design**
96 To determine lipidomic remodeling induced by environmental perturbations, we measured the
97 lipidomes of *M. extorquens* under physical and chemical challenges to cellular membrane
98 homeostasis (Figure 1a; Figure 1-Figure supplement 1). To this end, we varied temperature, osmotic
99 conditions, detergent stresses, carbon sources, and cell densities (Figure 1-Figure supplement 2).

100 Cells were harvested during early exponential growth to minimize their impact on media chemical
101 composition. Temperature was varied from 6 to 30 ˚C to challenge the viscosity of the membranes.
102 Salt (NaCl) and detergent (Triton X-100) concentrations were varied to produce osmotic and
103 detergent stresses, respectively. Cells were grown on two concentrations of methanol (0.1 and 1%
104 v/v) as the sole carbon source to evaluate the effect of metabolism on lipidomic remodeling. Finally,
105 to characterize lipidomic adaptation at varying cell densities, cells were harvested at early, mid and
106 late exponential, as well as stationary growth stages (Figure 1b). Cellular lipid content was analyzed
107 by high resolution shotgun mass spectrometry (Ejsing et al., 2009) to determine absolute abundances
108 of 25 phospholipids and two hopanoid species, distributed between 5 lipid classes and representing
109 over 90 mol% of the lipidome of *M. extorquens* (Sáenz et al., 2015)(Figure 2).
110
111 It has been previously shown that *M. extorquens* produces predominately lipids with 16 and 18 carbon
112 atoms-long acyl chains, and with up to 2 double bonds per acyl chain (Bradley et al., 2017; Wallace
113 et al., 1990). Consistently, the major PG, PE, and PC species have cumulative chain length of 36 or
114 34 carbons with two double bonds per lipid (e.g. 18:1/18:1 and 18:1/16:1) and minor species with up
115 to 4 double bonds per lipid. We also observed methylation of diplopterol (2Me-DIP) which has
116 previously been reported in cyanobacteria and methylotrophic bacteria including *Methylobacterium*
117 (Bradley et al., 2017; Rashby et al., 2007; Stampf et al., 1991; Summons et al., 1999). Recent work
118 suggests that 2-methylation may be particularly prevalent among plant-associated bacteria (Ricci et
119 al., 2014). In the following sections, we dissect the data in Figure 2 in order to reveal patterns in
120 lipidomic variation across experimental conditions.
121
122 **2.2 Lipidomic variation across experimental conditions**
123 To broadly characterize the effect of environmental perturbations on membrane remodeling, we
124 evaluated the cumulative lipid variability for each growth condition. Presently there is no gold
125 standard for evaluating lipidomic variability. Lipid variability has previously been reported as the
126 variance over mean of lipid abundance (Klose et al., 2012). This analysis reveals how much a lipid
127 varies relative to its abundance, such that even a very low abundance lipid that has a small change in
128 relation to a total lipidome could have a high variance over mean. However, in this study we aimed
129 to characterize variations that would have an impact on the bulk adaptive properties of the membrane.
130 Since small changes in abundance do not have a considerable effect on the bulk adaptive properties
131 of the membrane, we focused on lipids with high absolute changes in abundance. Therefore, we
132 calculated lipid variability as the standard deviation of abundances over a range of conditions. The
133 total lipidomic variability was then calculated as the aggregate standard deviation of relative

134 abundance for all individual lipid species over the range of the various conditions (e.g. temperature,
135 growth stage, etc.) (Figure 3a). This analysis revealed that temperature has by far the largest effect
136 on lipidomic remodeling, with more than 2-fold more variability than any other condition.
137 Surprisingly, the smallest effects were observed with detergent challenge.
138
139 To compare general lipidomic features for each individual experimental condition, we performed a
140 principle component analysis (PCA) on lipid species abundances (Figure 3b). PCA is a method that
141 allows for the comparison of multidimensional data by reducing variations down to two-dimensions
142 called principle components. Distance between each point on the PCA plot is proportional to variation
143 in lipid composition between conditions. Most conditions clustered closely with the standard growth
144 condition, shown in red. Thus, lipid composition was not strongly affected by detergent, methanol,
145 low salt concentrations, or during the progression through early, mid, and late growth stage. In stark
146 contrast, bacteria grown at low temperatures, in stationary growth phase, or at high salt conditions
147 (0.2 M NaCl) did not cluster with the standard growth condition, indicating a high extent of lipidome
148 remodeling. Furthermore, temperature had an orthogonal effect compared to stationary growth and
149 high salt conditions, indicating that a different set of lipidomic features is involved in responses to
150 those conditions.
151
152 It is surprising that a membrane destabilizing detergent (Helenius, 1975) did not result in lipidomic
153 remodeling. This could possibly be attributed to the ability of Gram-negative bacteria to resist
154 chemicals through the robustness imparted by barrier function of lipopolysaccharide at the cell
155 surface and active removal of toxins by multidrug transporters (Nikaido, 1996; 2003; Nikaido and
156 Vaara, 1985; Piddock, 2006). The insensitivity of the lipidome to methanol was also unexpected.
157 Klose et al. (2012) showed that the yeast lipidome varied greatly with differing carbon substrates
158 based on a similar PCA analysis. Our result suggests that methanol and succinate metabolism do not
159 require different membrane properties in *M. extorquens*. Nonetheless, the dominant effect of
160 temperature is consistent with the large diurnal temperature variations that *M. extorquens* must adjust
161 to in its native habitat on plant leaf surfaces and in soils. It is possible that the mechanisms of lipidome
162 adaptation and the lipidomic composition in *M. extorquens* have evolved to be particularly well-
163 suited for temperature changes.
164
165 **2.3 Variation in individual lipid species**
166 We next examined the individual lipid species involved in membrane adaptation in *M. extorquens*
167 (Figure 4). We again calculated individual lipid species as the standard deviation of abundances for

168 a given range of conditions (Figure 4b'). The highest abundance species generally show the largest
169 degree of variability (Figure 4a and 4b). However, there are some low abundance species that exhibit
170 large variations, notably lipids with 3 and 4 double bonds. An important point of emphasis is that low
171 abundance or undetectable species at standard growth conditions can become major components
172 under certain conditions, playing a crucial role in adaptation. The most striking result is that the
173 majority of lipid species do not vary substantially under any conditions, suggesting that only a small
174 fraction of the lipidome is required for adaptive membranes.
175
176 We then asked how many and which lipid species are highly variable for each set of conditions. We
177 defined the highly variable lipid species as those that account for 90% of the total lipidomic variability
178 within any given condition. By this measure we observed that 10-13 lipids are highly variable over
179 any given condition (Figure 4c), meaning that only around 30% of the lipidome is involved in
180 remodeling during adaptation. Of these 10-13 highly variable lipids, 8 are highly variable over all of
181 the conditions tested. These results revealed that only a fraction of the lipidome is involved in adaptive
182 remodeling and point towards the minimum complexity of lipid species required for membrane
183 adaptation. In principle, it is possible that as few as 8 lipid species could support adaptation over the
184 range of experimental conditions examined in this study.
185
186 **2.4 Variation of lipid structural features**
187 Membrane biophysical properties are modulated by changes in the abundance of lipid structural
188 features. For instance, increasing the number of double bonds per lipid reduces membrane viscosity
189 during adaptation to decreasing temperature, whereas various lipid headgroups can impart curvature
190 or surface charge. We analyzed how the various structural features of *M. extorquens* lipids are
191 modulated to glean insight into their sense and response mechanisms of membrane adaptation.
192
193 Headgroup features were differently regulated, as PC, PE and PG were relatively plastic, whereas CL
194 and diplopterols are relatively invariant (Figure 5a). For acyl chains, most of the variability is
195 observed for lipids with 2 and 3 double bonds and with total chain length of 34-36 carbons (Figure
196 5b). When we group acyl chain features separately for each headgroup (e.g. PC-specific unsaturation)
197 PC shows the largest variability for both unsaturation and chain length, whereas PG acyl chain
198 features are nearly invariant. This shows that acyl chain features are regulated independently within
199 each headgroup and provides a starting recipe for designing a responsive synthetic lipidome.
200

To assess how much different features varied for each experimental condition we calculated the variance of lipid features for each range of conditions as depicted by the heat map in Figure 5c. The highest variation in lipid classes is observed over temperature and growth stage. Interestingly, total lipid unsaturation varies over temperature but is relatively invariant over all other conditions. The most variation in total lipid chain length varies with temperature and salt concentration. These results reveal that membrane adaptation of total lipid features exhibit different patterns in response to different experimental conditions. This shows that the lipidomic adaptation mechanism is capable of unique, orthogonal responses to different perturbations.

2.5 Progressive remodeling of lipids across experimental conditions

Assessing lipidomic data for each step within each condition allows us to compare lipids as we go stepwise through the changes. For instance, how does the lipidome compare when the growth temperature is lowered from 30 to 20 to 13 and to 4 ˚C, or as cells progress from early to mid, to late and finally to stationary growth phase? We again consider lipids grouped by their features as this allowed us to monitor structural variations that directly impact the membrane's biophysical properties (Figure 6; Figure 6-Figure supplement 1-4).

Class

Lipid class abundances are relatively invariant over most conditions (Figure 6). PC abundance increases with decreasing temperature, with a pronounced change at 6 ˚C. PE abundance increases considerably when cells are in stationary growth stage. These results suggest that lipid class distribution is only adjusted under extreme conditions.

Double Bonds

The total number of double bonds per lipid varies substantially with temperature and is nearly invariant for other conditions (Figure 6a). As temperature decreases the abundances of DB3 and DB4 lipids increase, while abundances of DB1 and DB2 decrease. This contrasts with other organisms such as yeast where primarily DB1 and DB2 are adjusted with temperature change (Klose et al., 2012). It is possible that having additional double bonds enhances Methylobacterium's ability to adapt to broad temperatures that they experience on plant surfaces and in soils.

The variation of double bonds per lipid within each headgroup class is not evenly distributed across classes (Figure 6b). For instance, for varying temperatures PC shows the highest remodeling whereas PG is nearly invariant. Additionally, for varying salt and growth stages where total unsaturation has

235 little or negligible variability, class-specific PC-DB and CL-DB vary considerably. These variations
236 in PC-DB and CL-DB are nearly equal and opposite resulting in no apparent change in total DB
237 content.
238
239 *Chain length*
240 Total chain length is highly conserved across all conditions, and only varies substantially at 6 ˚C
241 (Figure 6a). Since total chain length has a large effect on membrane thickness, which in turn must be
242 matched with membrane proteins transmembrane domain length, it is not surprising that this feature
243 is so invariant. The large change in total CL at extreme low temperature suggests that the membrane
244 must take extreme measures to adapt as it approaches the end of the range of viable growth
245 temperature.
246
247 Similar to unsaturation, chain length within each headgroup class shows much higher variability than
248 total chain length (Figure 6b). For instance, from 30 to 20 ˚C total chain length remains constant
249 while PC chain length decreases and is compensated for by increased chain length in PG, PE and CL.
250 Similar remodeling is also observed for growth stage and salt concentration. Additionally, PC exhibits
251 the highest chain length variation.
252
253 *Diplopterol 2-methylation*
254 A particularly striking variation was observed for the sterol analogue diplopterol and its 2-methylated
255 derivative (Figure 7). Diplopterol is the major hopanoid in *M. extorquens* and is localized in the outer
256 membrane (Hancock and Williams, 1986; Sáenz et al., 2015). We previously demonstrated that
257 diplopterol has a sterol-like ability to modulate the order of saturated lipids such as
258 lipopolysaccharides in the bacterial outer membrane (Sáenz et al., 2012). Subsequent work
259 demonstrated that 2-methylation of hopanoids increases their membrane rigidifying effect (Sáenz et
260 al., 2015; Wu et al., 2015). Therefore, variations in diplopterol 2-methylation could play a role in the
261 adaptation of the outer membrane. While total diplopterol abundances (diplopterol + 2-methyl-
262 diplopterol) did not vary substantially under any conditions, 2-methylation of diplopterol is highly
263 variable in all conditions except methanol and detergent (Figure 7a and b). There is a progressive
264 increase in 2-methyl-diplopterol abundance with decreasing temperature and increasing salt
265 concentration (Figure 7c), consistent with transcriptional regulation of this process by global stress
266 response pathways (Kulkarni et al., 2013). These results show for the first time that 2-methylation is
267 dynamically regulated in response to varying growth conditions and is important for outer membrane
268 adaptation.

269

270 Our observations highlight three characteristics of structural lipid adaptation. First, we observed that
271 adaptivity of features over a particular range of conditions (e.g. temperature) does not involve a
272 monotonic pattern of feature remodeling, but rather can involve different features over intervals of a
273 given condition. Second, certain features such as acyl chain unsaturation and diplopterol 2-
274 methylation are highly variable and are remodeled over a broad range of conditions. However, other
275 features such as lipid class and acyl chain length are relatively invariant except under extreme
276 conditions of low temperature and stationary growth stage, suggesting that chain length and
277 headgroup distribution have multiple constraints (e.g. maintaining membrane thickness or surface
278 charge). Notably, even the tightly constrained features are adjusted under extreme perturbations.
279 Third, acyl chain features are regulated independently within each headgroup class. Thus, even when
280 total acyl chain unsaturation and length appears invariant, there can be extensive acyl chain
281 remodeling within specific headgroup classes. Such class-specific remodeling of unsaturation may
282 result in adaptation that is localized to the inner or outer membrane, or to specific regions within each
283 membrane, such as highly curved regions at the poles, one particular membrane leaflet, lipids that are
284 closely associated with protein transmembrane domains, or potentially lateral membrane domains.
285 On the other hand, constraining total unsaturation while internally shifting double bonds from PC to
286 CL might be a means of varying intrinsic curvature while maintaining total membrane viscosity.
287

288 **Summary and Outlook**

289 In this study, we systematically characterized the lipidome of *M. extorquens* over a range of growth
290 conditions to gain insights into membrane homeostatic adaptation. We demonstrated that membranes
291 composed of only a few lipid species are capable of adapting specifically to a broad range of
292 conditions, in particular temperature. Lastly, we showed that lipidomes must be assessed by lipid
293 species composition, but also by the composite structural features conferred by binned combinations
294 of lipids, such as the total number of double bonds or the global sum of acyl chain lengths, since
295 combination of these structural features ultimately dictates the physical state and functionality of
296 membranes.
297

298 We probed the lipidome composition across a broad range of viable conditions spanning temperature,
299 hyperosmotic and detergent stress, carbon sources, and cell density. While individual lipid species do
300 adapt to changing conditions, eight lipid species are variable in all experimental regimes (Figure 4)
301 and the majority of lipids remained surprisingly stable. PCA analysis reveals that most lipidomes are
302 highly similar across conditions (Figure 3). This demonstrates that the lipidome is robust and that

303 there are strong constraints on lipidome composition and remodelling. One of the outstanding
304 conundrums in membrane biology is to understand why there are so many lipids (Dowhan, 1997;
305 2017), even a relatively simple organism like *E. coli* has over 100 phospholipid species (Jeucken et
306 al., 2019). Recapitulating such a complex system from first principles seems daunting. However, the
307 lipidome of *M. extorquens* demonstrates that a synthetic membrane capable of supporting life over a
308 broad range of environmental conditions could be constructed with a relatively small number of lipid
309 species.
310
311 The lipidome adaptability is also constrained by structural elements of individual lipids. Instead of
312 analysing lipidomes purely by lipid species, it is therefore critical to assess the global structural
313 composition. For example, total phospholipid chain length, that influences membrane thickness, is a
314 highly conserved feature that only varies under extreme conditions such as low temperature (Jensen
315 and Mouritsen, 2004). Interestingly, phospholipid acyl chain length was highly conserved globally,
316 but variable within certain headgroup classes. Other constraints do not have such clear implications.
317 For instance, phospholipid headgroup composition only varies at low temperature or in stationary
318 growth phase, possibly suggesting conservation of membrane surface charge as a key constraint.
319 Also, the acyl chain composition among phospholipids with PG headgroup is nearly invariant across
320 all conditions, suggesting that there could be biochemical constraints on PG remodelling. Low PG
321 remodelling has also been observed in cyanobacteria (Pittera et al., 2018), showing that this constraint
322 is not limited to *M. extorquens*. In contrast, we learned that PC acyl chain composition is highly
323 variable and appears to take on the brunt of adaptive remodelling. While the physicochemical and
324 physiological basis for these observations remains to be fully explored, the patterns and constraints
325 in lipidome remodelling that we report here serve as a resource for designing a minimal adaptive
326 membrane and highlight the need for multi-level analysis of lipidome data.
327
328 Understanding how *M. extorquens* adapts with so few lipids, and even fewer that are responsive,
329 remains an open challenge. In particular, given that lipid remodelling did not involve a monotonic
330 change, but rather seemed to involve different features varying over different intervals of a given
331 range of conditions, such as temperature. One possibility is that the presence of isoprenoids, sterol-
332 like hopanoids, buffer changes in membrane properties and thereby minimizes the need for
333 phospholipid remodelling. Our previous data, however, shows that hopanoids primarily interact with
334 lipopolysaccharides in the outer leaflet of the outer membrane, and thus would not be relevant to
335 variations of the phospholipidome within the inner membrane or inner leaflet of the outer membrane
336 (Sáenz et al., 2015; 2012). Alternatively, it has also been proposed that in bacterial membranes

lacking sterol analogues or complex lipidomes, integral membrane proteins may serve a role in adaptation (Kaiser et al., 2011). Similarly unexplored are the sense and response pathways that underlie such complex patterns of lipidome adaptation. It has emerged in recent years that there can be dedicated membrane sensors, which are involved in regulating lipid biosynthesis pathways in response to perturbed membrane properties (Ernst et al., 2016; Puth et al., 2015; Saita and de Mendoza, 2015). It is presently unknown how many different sensors are required for adaptation, and how many orthogonal parameters can be distinguished by such sensors. Building on the lipidomic resource presented here, *M. extorquens* is a promising model organism to explore minimal mechanisms for cell membrane adaptation. The adaptive lipidome of *M. extorquens* provides a critical resource as a starting point to elucidate the regulatory systems underlying membrane adaptation.

Acknowledgements

The authors wish to thank Kai Simons and Robert Ernst for advice, members of Sáenz group for discussions, Michael Schlierf, Ilya Levental, Alex Bradley, Carl Modes, and Christoph Zechner for manuscript comments, and Lipotype GmbH.

Author contributions

Sandra Rizk and Daniel Grosser performed bacterial growth experiments. Oksana Lavrynenko performed MS analysis. Grzegorz Chwastek contributed to writing, editing and data analysis. Michał Surma performed MS data analysis and editing. Magda Rucińska performed bioinformatics analysis. Helena Jambor conceived and designed the figures. James Sáenz conceived the project, obtained funding, supervised the project, and wrote the manuscript. All authors read, edited and approved the final manuscript.

Funding

This work was supported by the B CUBE of the TU Dresden, a Simons Foundation Fellowship (to JPS), a German Federal Ministry of Education and Research BMBF grant (to JPS, project # 03Z22EN12), and a VW Foundation “Life” grant (to JPS, project # 93089).

367 **Methods**

368

369 **Media, growth conditions**

370 For all cultivations a defined media, here referred to as Hypho-TMM, was used (Delaney et al., 2013).
371 All liquid cultures were grown at 30 ˚C and pH 7 with shaking at 150 rpm unless stated otherwise.
372 For all experiments we used a strain of *M. extorquens PA1* with the cellulose synthase genes knocked
373 out to minimize clumping and improve cell density measurements (Delaney et al., 2013). Cultures
374 were started from a glycerol stock stored at -80 ˚C and were plated on Hypho-TMM agarose plate
375 and grown at 30 ˚C. A liquid pre-culture was set up by sterile picking a single colony and transferring
376 it to 5 ml of Hypho-TMM. This pre-culture was grown over night to near stationary phase. The
377 experimental culture was started by inoculation to $OD_{600\ nm}$ 0.02 with pre-culture and grown until a
378 final $OD_{600\ nm}$ of 0.2 – 0.3 (early log-phase) was reached. Several conditions were tested including
379 the influence of salinity, carbon source (MeOH and succinate), detergent (up to 5% Triton X-100)
380 and temperature (6 – 30 ˚C). Cells were also harvested at mid-, late- and stationary growth stages. A
381 defined volume representing 6 OD units (1 OD unit = 1 mL of OD 1) was sampled and pelleted. The
382 harvested cells were washed twice with fresh media. The pellet was snap frozen in liquid nitrogen
383 and stored until further processing at -20 ˚C.

384

385 *Hypho-TMM recipe:*

386 1.45 mM K_2HPO_4; 1.88 mM NaH_2PO_4; 45.6 µM sodium citrate; 1.2 µM $ZnSO_4$; 1 µM $MnCl_2$;
387 18 µM $FeSO_4$; 2 µM $(NH_4)_6Mo_7O_{24}$; 1 µM $CuSO_4$; 2 µM $CoCl_2$; Na_2WO_4; 0.5 mM $MgCl_2$;
388 8 mM $(NH_4)_2SO_4$; 20 µM $CaCl_2$
389 30 mM PIPES pH 7
390 15 mM succinate unless stated otherwise

391

392 **Shotgun mass spectrometry**

393 For the lipidomic analysis by mass spectrometry the lipids of harvested cells were extracted twice by
394 the method of Blight and Dyer (Bligh and Dyer, 1959). The total lipid extracts representing 6 OD
395 units of *M. extorquens* were analysed by quantitative shotgun lipidomics (Ejsing et al., 2009) adapted
396 for the quantification of hopanoids (diplopterol and 2-methyl-diplopterol).

397

398 *Measurement of phospholipids*

399 For absolute quantification extracts were diluted with MS mix (7.5 mM ammonium acetate in
400 isopropanol/methanol/chloroform 4:2:1) containing the 0.5 µM PC (34:0), PE (34:0), PG (34:0)

401 mixture and 0.05 µM CL (57:4). MS spectra were acquired on Q Exactive tandem mass spectrometer
402 (Thermo Fisher Scientific, Bremen, Germany) equipped with a robotic nanoflow ion source TriVersa
403 NanoMate (Advion BioSciences, Ithaca NY). Spectra were acquired in negative MS mode with the
404 mass resolution of $R_{m/z\ 400}$ = 280000 with AGC target value of 10^6 and maximum injection time of 1
405 s in the range of masses 400 – 1000 m/z. Raw data were processed using LipidXplorer software
406 (Herzog et al., 2012; 2011). Based on high accuracy and resolution masses, species belonging to 4
407 phospholipid classes including phosphatidylcholine (PC), monitored as an acetate adduct,
408 phosphatidylethanolamine (PE), phosphatidylglycerol (PG), both monitored as deprotonated anions,
409 and cardiolipin (CL), monitored as a doubly deprotonated anion, were identified.
410
411 *Measurement of diplopterol*
412 The extract was dried down and re-dissolved in MS mix (7.5 mM ammonium acetate in
413 isopropanol/methanol/chloroform 4:2:1) containing the 0.13 mM cholesterol D7 standard. MS
414 spectra were acquired on Q Exactive tandem mass spectrometer (Thermo Fisher Scientific, Bremen,
415 Germany) equipped with a robotic nanoflow ion source TriVersa NanoMate (Advion BioSciences,
416 Ithaca NY). Spectra were acquired in positive MS mode with the mass resolution of $R_{m/z\ 400}$ = 140000
417 with AGC target value of 10^6 and maximum injection time of 1 s in the range of masses 360 – 455
418 m/z. Raw data were processed using LipidXplorer software. Diplopterol and 2-methyl-diplopterol
419 were monitored as M - $[H_2O]$ + H^+ ... and cholesterol D7 as M - $[H_2O]$ + H^+. Absolute concentrations
420 of diplopterol and methyl-diplopterol were determined using calibration curves and response factors
421 established alongside with cholesterol D7 and purified diplopterol mixed at various ratios.
422
423 **Data analysis**
424 Lipid abundances (mol% of total) of biological triplicates for all conditions are provided in the
425 supplementary materials. One of the replicates at 13 ˚C and at TX-100 1% yielded erroneous
426 abundance data due to a problem with the internal standard in those replicates and we have therefore
427 excluded them from our analyses.
428
429 Variation of lipid species across experimental conditions was calculated by taking the standard
430 deviation of lipid abundances for replicates over a given range of conditions (e.g. temperature, salt,
431 etc.). Total lipidomic variation was calculated as the cumulative variation of individual lipid species
432 for a given range of conditions.
433

Visualization of lipidome variation for all conditions was investigated with principle component analysis (PCA). PCA was performed by using the R prcomp function in RStudio with default parameters, where the calculation is carried out by a singular value decomposition of the (centered and scaled) data matrix. Visualization in single plots performed using the ggbiplot function. PCA allows the identification of latent variables (principal components) in the data based on 14 observed variables. The plot is based on principal components 1 and 2, which explain 50.1% and 16.5% of the total variance of the data, respectively.

Variations in abundance of lipid features were analysed by binning lipid species according to structural features including total chain length, saturation, class (e.g. phospholipid headgroup and diplopterols), and 2-methylation of diplopterol. Acyl chain length and saturation were binned for all phospholipids (global acyl chain features), and separately within each headgroup (headgroup specific acyl chain features).

Figure Captions

Figure 1. Overview of experimental outline and lipids analysed in this study. (A) Overview of experimental design and exemplary data obtained. **(B)** Schematic of lipid structural features measured in this study: headgroups of phospholipids and isoprenoids, acyl chain length and acyl chain saturation (number of double bonds).

Figure 1-figure supplement 1. Bacterial growth rates (Herbert et al., 1956) for all experimental conditions.

Figure 2. Table of lipid species abundances. Lipid species are annotated by class/headgroup (PG, PE, PC, CL or diplopterol), total acyl chain length (32 to 72), and total acyl chain saturation (number of double bonds per lipid, 0 to 4). Abundance is shown as percentage of total lipids per experiment. The range in abundance across all experimental conditions is indicated by individual grey dots, the abundances for the standard growth condition (30 ˚C, early exponential stage, 0.15 M sucrose) are shown in red.

Figure 3. Effect of experimental conditions on lipidomic variability. (A) Total lipidomic variability is given as the cumulative standard deviation of individual lipid species across each set of experimental conditions. Lipid variability is highest when varying temperature, and lowest in increasing percentage of detergent. **(B)** Principle component analysis (PCA) of the lipid species abundances shows the degree of variation between subconditions. The standard growth condition (30 ˚C, early exponential stage, 0.15 M sucrose) is indicated in red, and all other subconditions are grey. Again, lipidomes vary greatly in changing temperatures regimes, and also when bacteria enter stationary phase growth.

Figure 4. Variability of individual lipid species across experimental conditions. (A) Average abundances of lipid species for all conditions sorted from highest (PG 36:2) to lowest (CL 64:0) lipid species. Mean and range are shown for each lipid. **(B)** Heat map of lipid species variability across experimental conditions, high variability is indicated in red, no variability in light yellow. **(B')** Exemplary calculation of standard deviation. **(C)** UpSetR plot (Conway et al., 2017) showing the overlap of lipids adapting their amounts across the experimental conditions. Eight lipids vary their abundance in all experimental conditions, four lipids vary abundance specifically in changing temperatures. Stage: bacterial growth stage/phase, TX: varying detergent concentrations.

Figure 5. Variability of phospholipid structural features across experimental conditions. (A) Abundances of lipids grouped by lipid class shows overall low variability, and lowest variability of CL. **(B)** Abundances of phospholipid headgroup binned by acyl chain length and acyl chain saturation respectively reveals group specific differences in acyl chain remodeling. (headgroups: blue = PG, green = PE, olive = PC, magenta = CL). **(A), (B)** each data point shows lipid abundance from individual biological replicates. **(C)** Variability of lipid features plotted for each set of experimental conditions. Stage: bacterial growth stage/phase, TX: varying detergent concentrations.

Figure 6. Step-wise adaptation of lipids by feature at changing environmental growth conditions. (A) Abundances of lipids grouped by class, acyl chain length and acyl chain saturation when changing growth temperature, probing at different growth stages, and varying salt (NaCl) concentration of the growth media. **(B)** Abundances of phospholipids grouped by acyl chain features, with headgroups indicated by color (blue: PG, green: PE, olive: PC, magenta: CL). This reveals compensatory effects in lipid adaptability: while abundance of PC with 2 double bonds increases with

increasing temperatures, PC with 3 double bonds decreases from 6 to 30 ˚C. In each panel, the most variable features are highlighted in bold.

Figure 7. Diplopterol (hopanoid) methylation (A) Abundances of diplopterol species across growth conditions. **(B)** Step-wise adaptation of diplopterols when changing temperature, growth phase, and salt condition.

Figure 1 – Supplement 1 Graphical abstract
Figure 1 – Supplement 2 Bacterial growth curves and sampling points for lipidomic analysis. Chart for growth phases is a conceptual drawing.
Figure 6 – Supplement 1 Overview of compositional changes across exemplary experimental conditions reveals the lipidome is robust in most growth conditions except in drastic temperature changes when the lipidome is markedly different.
Figure 6 – Supplement 2. Step-wise adaptation of lipids by feature sampled at varying growth temperatures.
Figure 6 – Supplement 3. Step-wise adaptation of lipids by feature sampled at early, late, mid and stationary growth phase.
Figure 6 – Supplement 4. Step-wise adaptation of lipids by feature sampled at varying salt concentrations (NaCl).

527 **References**
528
529 Bligh, E.G., and Dyer, W.J. (1959). A Rapid Method of Total Lipid Extraction and Purification.
530 Canadian Journal of Biochemistry and Physiology *37*, 911–917.

531 Bradley, A.S., Swanson, P.K., Muller, E.E.L., Bringel, F., Caroll, S.M., Pearson, A., Vuilleumier,
532 S., and Marx, C.J. (2017). Hopanoid-free Methylobacterium extorquens DM4 overproduces
533 carotenoids and has widespread growth impairment. PLoS ONE *12*, e0173323.

534 Brea, R.J., Rudd, A.K., and Devaraj, N.K. (2016). Nonenzymatic biomimetic remodeling of
535 phospholipids in synthetic liposomes. P Natl Acad Sci Usa *113*, 8589–8594.

536 Buddingh, B.C., and van Hest, J.C.M. (2017). Artificial Cells: Synthetic Compartments with Life-
537 like Functionality and Adaptivity. Acc. Chem. Res *50*, 769–777.

538 Conway, J.R., Lex, A., and Gehlenborg, N. (2017). UpSetR: an R package for the visualization of
539 intersecting sets and their properties. Bioinformatics *33*, 2938–2940.

540 Delaney, N.F., Kaczmarek, M.E., Ward, L.M., Swanson, P.K., Lee, M.C., and Marx, C.J. (2013).
541 Development of an optimized medium, strain and high-throughput culturing methods for
542 Methylobacterium extorquens. PLoS ONE *8*, e62957.

543 Dowhan, W. (1997). Molecular basis for membrane phospholipid diversity: why are there so many
544 lipids? Annu Rev Biochem. *66*, 199-232.
545

546 Dowhan, W. (2017). Understanding phospholipid function: Why are there so many lipids? J. Biol.
547 Chem. *292*, 10755–10766.

548 Ejsing, C.S., Sampaio, J.L., Surendranath, V., Duchoslav, E., Ekroos, K., Klemm, R.W., Simons,
549 K., and Shevchenko, A. (2009). Global analysis of the yeast lipidome by quantitative shotgun mass
550 spectrometry. Proceedings of the National Academy of Sciences *106*, 2136–2141.

551 Ernst, R., Ejsing, C.S., and Antonny, B. (2016). Homeoviscous Adaptation and the Regulation of
552 Membrane Lipids. Journal of Molecular Biology *428*, 4776–4791.

553 Gorter, E., and Grendel, F. (1925). On biomolecular layers of lipoids on the chromocytes of the
554 blood. J Exp Med *41*, 439–443.

555 Hancock, I., and Williams, K. (1986). The outer membrane of Methylobacterium organophilum.
556 Journal of General Microbiology *132*, 599-610.
557

558 Hardy, M.D., Yang, J., Selimkhanov, J., Cole, C.M., Tsimring, L.S., and Devaraj, N.K. (2015).
559 Self-reproducing catalyst drives repeated phospholipid synthesis and membrane growth. P Natl
560 Acad Sci Usa *112*, 8187–8192.

561 Helenius, A. (1975). Solubilization of membranes by detergents. Biochim Biophys Acta *415(1)*, 29-
562 79.

563 Herzog, R., Schuhmann, K., Schwudke, D., Sampaio, J.L., Bornstein, S.R., Schroeder, M., and
564 Shevchenko, A. (2012). LipidXplorer: A Software for Consensual Cross-Platform Lipidomics.
565 PLoS ONE *7*, e29851.

566 Herzog, R., Schwudke, D., Schuhmann, K., Sampaio, J.L., Bornstein, S.R., Schroeder, M., and
567 Shevchenko, A. (2011). A novel informatics concept for high-throughput shotgun lipidomics based
568 on the molecular fragmentation query language. Genome Biol. *12*, R8.

569 Hunte, C., and Richers, S. (2008). Lipids and membrane protein structures. Curr Opin Struct Biol
570 *18*, 406–411.

571 Jensen, M., and Mouritsen, O. (2004). Lipids do influence protein function - the hydrophobic
572 matching hypothesis revisited. BBA-Biomembranes *1666*, 205–226.

573 Jeucken, A., Molenaar, M.R., van de Lest, C.H.A., Jansen, J.W.A., Helms, J.B., and Brouwers, J.F.
574 (2019). A Comprehensive Functional Characterization of Escherichia coli Lipid Genes. Cell Rep
575 *27*, 1597–1606.e2.

576 Kaiser, H.-J., Surma, M.A., Mayer, F., Levental, I., Grzybek, M., Klemm, R.W., Da Cruz, S.,
577 Meisinger, C., Müller, V., Simons, K., et al. (2011). Molecular Convergence of Bacterial and
578 Eukaryotic Surface Order. J Biol Chem *286*, 40631–40637.

579 Klose, C., Surma, M.A., and Simons, K. (2013). Organellar lipidomics-background and
580 perspectives. Curr Opin Cell Biol *25(4)*, 406-13.

581 Klose, C., Surma, M.A., Gerl, M.J., Meyenhofer, F., Shevchenko, A., and Simons, K. (2012).
582 Flexibility of a Eukaryotic Lipidome – Insights from Yeast Lipidomics. PLoS ONE *7*, e35063.

583 Kulkarni, G., Wu, C.-H., and Newman, D.K. (2013). The General Stress Response Factor EcfG
584 Regulates Expression of the C-2 Hopanoid Methylase HpnP in *Rhodopseudomonas palustris* TIE-1.
585 J Bacteriol *195*, 2490–2498.

586 Levental, K.R., Lorent, J.H., Lin, X., Skinkle, A.D., Surma, M.A., Stockenbojer, E.A., Gorfe, A.A.,
587 and Levental, I. (2016). Polyunsaturated Lipids Regulate Membrane Domain Stability by Tuning
588 Membrane Order. Biophys J *110*, 1800–1810.

589 Nikaido, H. (1996). Multidrug efflux pumps of gram-negative bacteria. J Bacteriol *178*, 5853–5859.

590 Nikaido, H. (2003). Molecular basis of bacterial outer membrane permeability revisited.
591 Microbiology and Molecular Biology Reviews *67*, 593–656.

592 Nikaido, H., and Vaara, M. (1985). Molecular-Basis of Bacterial Outer-Membrane Permeability.
593 Microbiol Rev *49*, 1–32.

594 Piddock, L.J.V. (2006). Multidrug-resistance efflux pumps - not just for resistance. Nat Rev Micro
595 *4*, 629–636.

596 Pittera, J., Jouhet, J., Breton, S., Garczarek, L., Partensky, F., Maréchal, É., Nguyen, N.A., Doré,
597 H., Ratin, M., Pitt, F.D., et al. (2018). Thermoacclimation and genome adaptation of the membrane
598 lipidome in marine Synechococcus. Environ Microbiol *20*, 612–631.

599 Pomorski, T., and Menon, A.K. (2006). Lipid flippases and their biological functions. Cell Mol Life
600 Sci *63*, 2908–2921.

601 Puth, K., Hofbauer, H.F., Sáenz, J.P., and Ernst, R. (2015). Homeostatic control of biological
602 membranes by dedicated lipid and membrane packing sensors. Biol Chem *396*, 1043–1058.

603 Rashby, S.E., Sessions, A.L., Summons, R.E., and Newman, D.K. (2007). Biosynthesis of 2-
604 methylbacteriohopanepolyols by an anoxygenic phototroph. Proceedings of the National Academy
605 of Sciences *104*, 15099–15104.

606 Ricci, J.N., Coleman, M.L., Welander, P.V., Sessions, A.L., Summons, R.E., Spear, J.R., and
607 Newman, D.K. (2014). Diverse capacity for 2-methylhopanoid production correlates with a specific
608 ecological niche. The ISME Journal *8*, 675–684.

609 Saita, E.A., and de Mendoza, D. (2015). Thermosensing via transmembrane protein–lipid
610 interactions. Biochimica Et Biophysica Acta (BBA)-Biomembranes *1848*, 1757–1764.

611 Sampaio, J.L., Gerl, M.J., Klose, C., Ejsing, C.S., Beug, H., Simons, K., and Shevchenko, A.
612 (2011). Membrane lipidome of an epithelial cell line. P Natl Acad Sci Usa *108*, 1903–1907.

613 Sanders, C.R., and Mittendorf, K.F. (2011). Tolerance to Changes in Membrane Lipid Composition
614 as a Selected Trait of Membrane Proteins. Biochemistry *50*, 7858–7867.

615 Sáenz, J.P., Grosser, D., Bradley, A.S., Lagny, T.J., Lavrynenko, O., Broda, M., and Simons, K.
616 (2015). Hopanoids as functional analogues of cholesterol in bacterial membranes. P Natl Acad Sci
617 Usa *112*, 11971–11976.

618 Sáenz, J.P., Sezgin, E., Schwille, P., and Simons, K. (2012). Functional convergence of hopanoids
619 and sterols in membrane ordering. Proceedings of the National Academy of Sciences *109*, 14236–
620 14240.

621 Singer, S.J., and Nicolson, G.L. (1972). The fluid mosaic model of the structure of cell membranes.
622 Science *175*, 720–731.

623 Stampf, P., Herrmann, D., Bisseret, P., and Rohmer, M. (1991). 2α-Methylhopanoids: First
624 Recognition in the Bacterium Methylobacterium organophilum and Obtention via Sulphur Induced
625 Isomerization of 2ß-Methylhopanoids. Tetrahedron *47*, 7081–7090.

626 Summons, R.E., Jahnke, L.L., Hope, J.M., and Logan, G.A. (1999). 2-Methylhopanoids as
627 biomarkers for cyanobacterial oxygenic photosynthesis. Nature *400*, 554–557.

628 Tang, D., Rohaida Che Hak, C., Thompson, A.J., Kuimova, M.K., Williams, D.S., Perriman, A.W.,
629 and Mann, S. (2014). Fatty acid membrane assembly on coacervate microdroplets as a step towards
630 a hybrid protocell model. Nature Chemistry *6*, 527–533.

631 van Meer, G., Voelker, D.R., and Feigenson, G.W. (2008). Membrane lipids: where they are and
632 how they behave. Nat Rev Mol Cell Bio *9*, 112–124.

633 Wallace, P., Hollis, D., and Weaver, R. (1990). Biochemical and chemical characterization of pink-
634 pigmented oxidative bacteria. J Clin Microbiol *28(4)*, 689–693.

635 Wu, C.-H., Bialecka-Fornal, M., and Newman, D.K. (2015). Methylation at the C-2 position of
636 hopanoids increases rigidity in native bacterial membranes. eLife *4*, e05663.

637

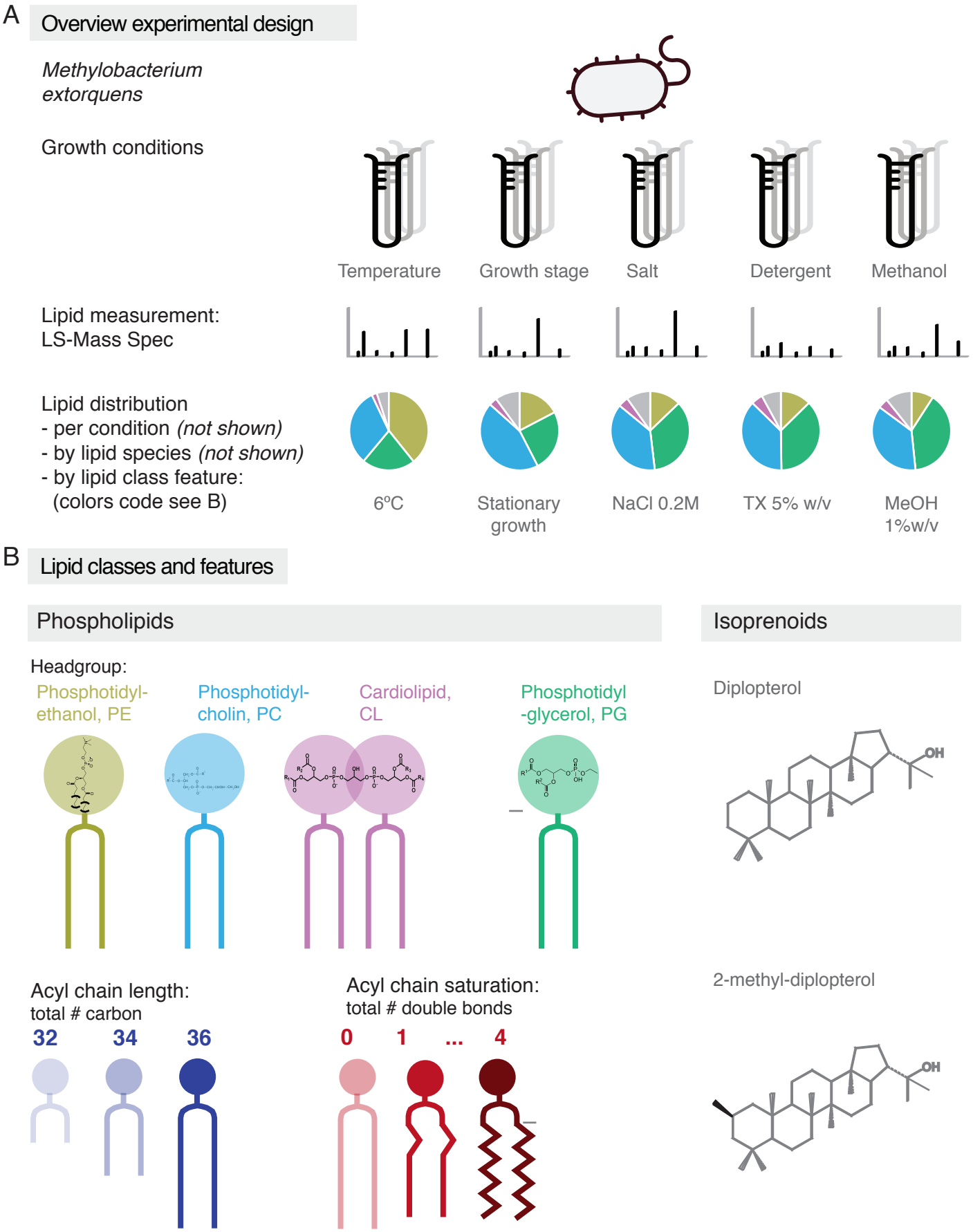

Figure 1. Overview of experimental outline and lipids analysed in this study. (A) Overview of experimental design and exemplary data obtained. **(B)** Schematic of lipid structural features measured in this study: head groups of phosopholipids and isoprenoids, acyl chain length and acyl chain saturation (number of double bonds).

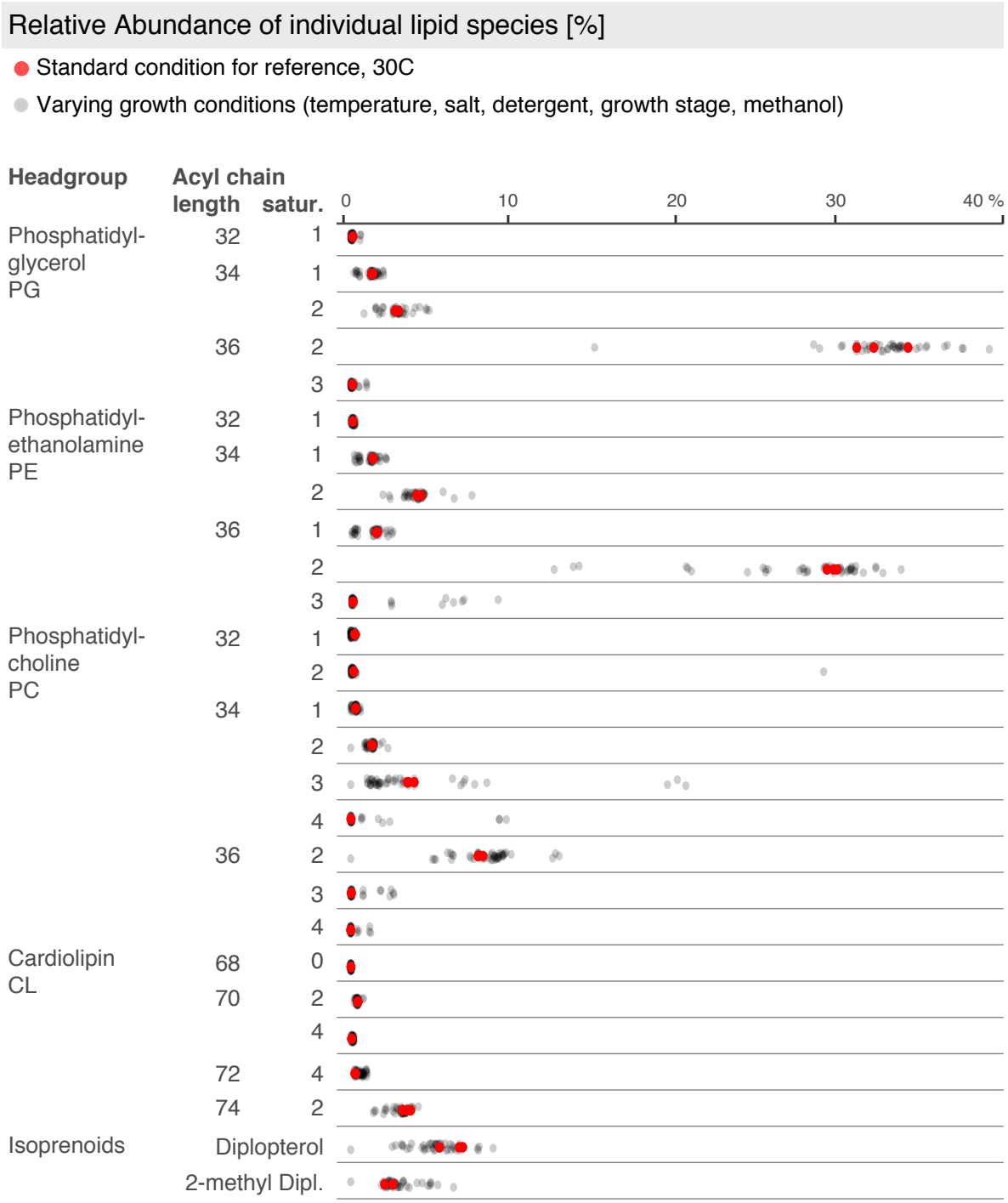

Figure 2. Table of lipid species abundances. Lipid species are annotated by class/head group (PG, PE, PC, CL or diplopterol), total acyl chain length (32 to 74), and total acyl chain saturation (number of double bonds per lipid, 0 to 4). Abundance is shown as percentage of total lipids per experiment. The range in abundance across all experimental conditions is indicated by individual grey dots, the abundances for the standard growth condition (30 ˚C, early exponential stage, 0.15 M sucrose) are shown in red.

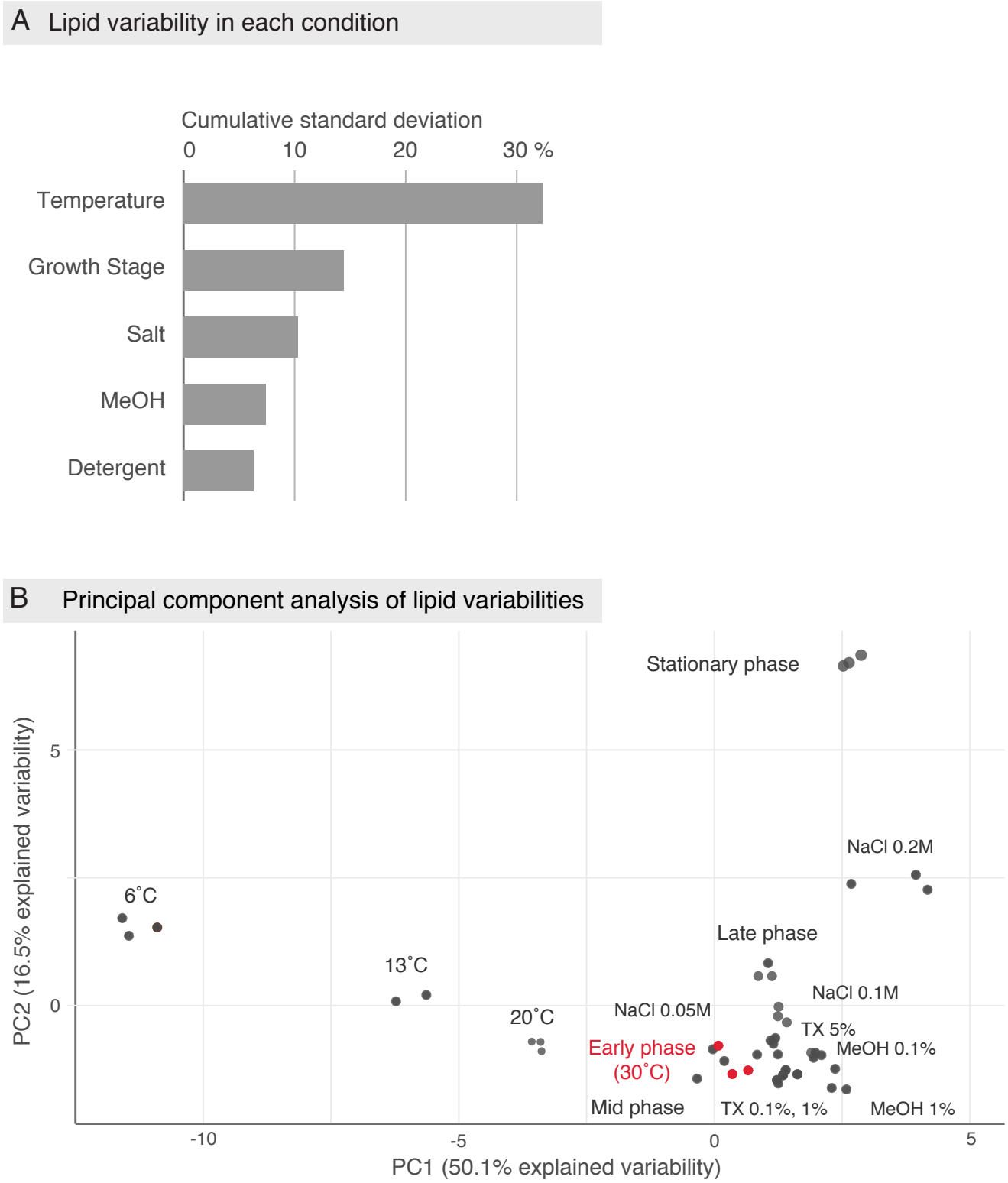

Figure 3. Effect of experimental conditions on lipidomic variability. (A) Total lipidomic variability is given as the cumulative standard deviation of individual lipid species across each set of experimental conditions. Lipid variability is highest when varying temperature, and lowest in increasing percentage of detergent. **(B)** Principle component analysis (PCA) of the lipid species abundances shows the degree of variation between subconditions. The standard growth condition (30 ˚C, early exponential stage, 0.15 M sucrose) is indicated in red, and all other subconditions are grey. Again, lipidomes vary greatly in changing temperatures regimes, and also when bacteria enter stationary phase growth. TX = detergent

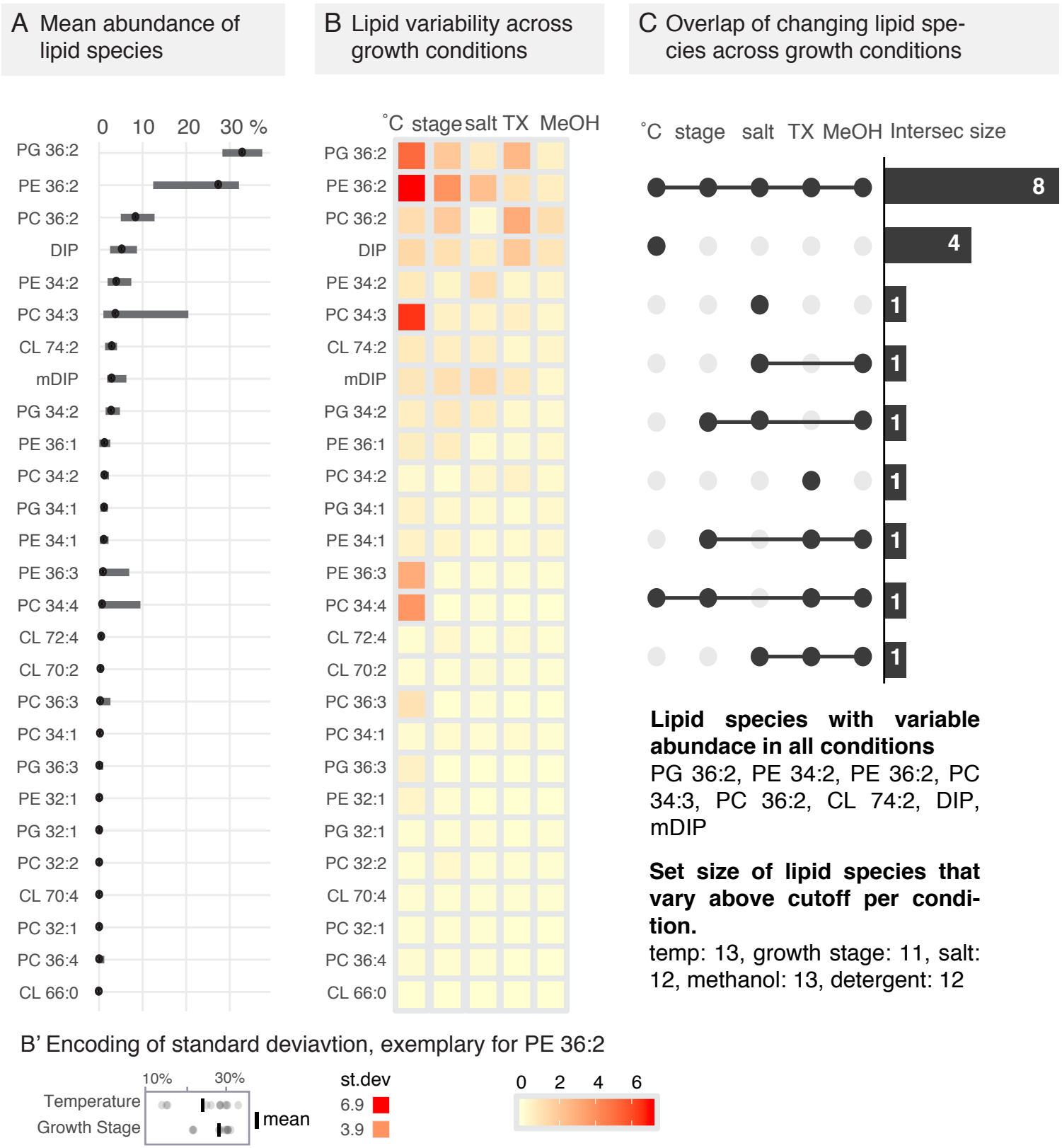

Figure 4. Variability of individual lipid species across experimental conditions. (A) Average abundances of lipid species for all conditions sorted from highest (PG 36:2) to lowest (CL 66:0) lipid species. Mean and range are shown for each lipid. **(B)** Heat map of lipid species variability across experimental conditions, high variability is indicated in red, no variability in light yellow. (B') Exemplary calculation of standard deviation. **(C)** UpSetR plot (Conway, 2017) showing the overlap of lipids adapting their amounts across the experimental conditions. Eight lipids vary their abundance in all experimental conditions, four lipids vary abundance specifically in changing temperatures. stage = growth stage/phase, TX = varying detergent concentrations.

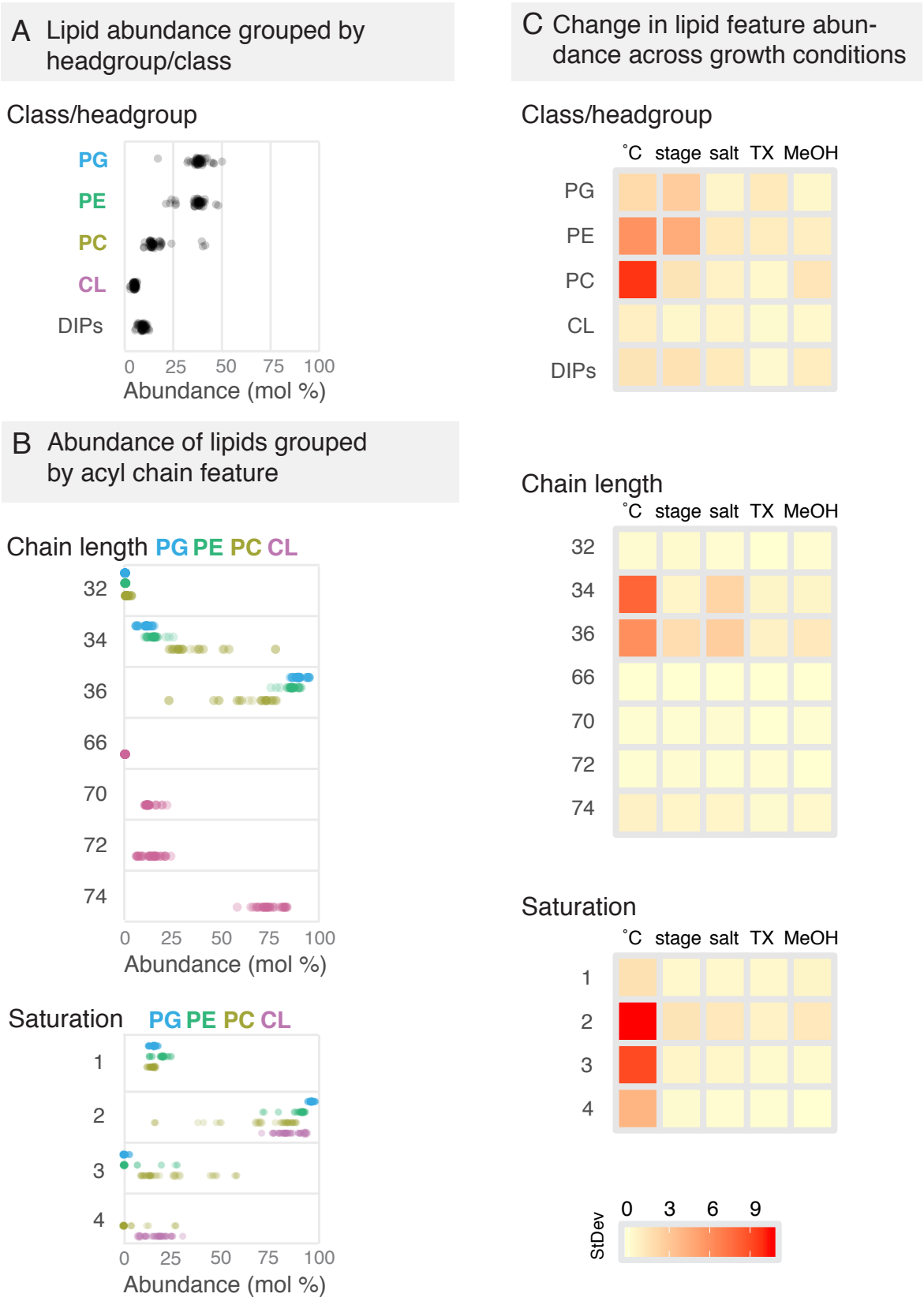

Figure 5. Variability of phospholipid structural features across experimental conditions. **(A)** Abundances of lipids grouped by lipid class shows overall low variability, and lowest variability of CL. **(B)** Abundances of phospholipid headgroup binned by acyl chain length and acyl chain saturation respectively reveals group specific differences in acyl chain remodelling. (headgroups blue = PG, green = PE, olive = PC, magenta = CL). **(A), (B)** each data point shows mean lipid amount from three biological replicates. **(C)** Variability of lipid features plotted for each set of experimental conditions. Stage: bacterial growth stage/phase, TX: varying detergent concentrations.

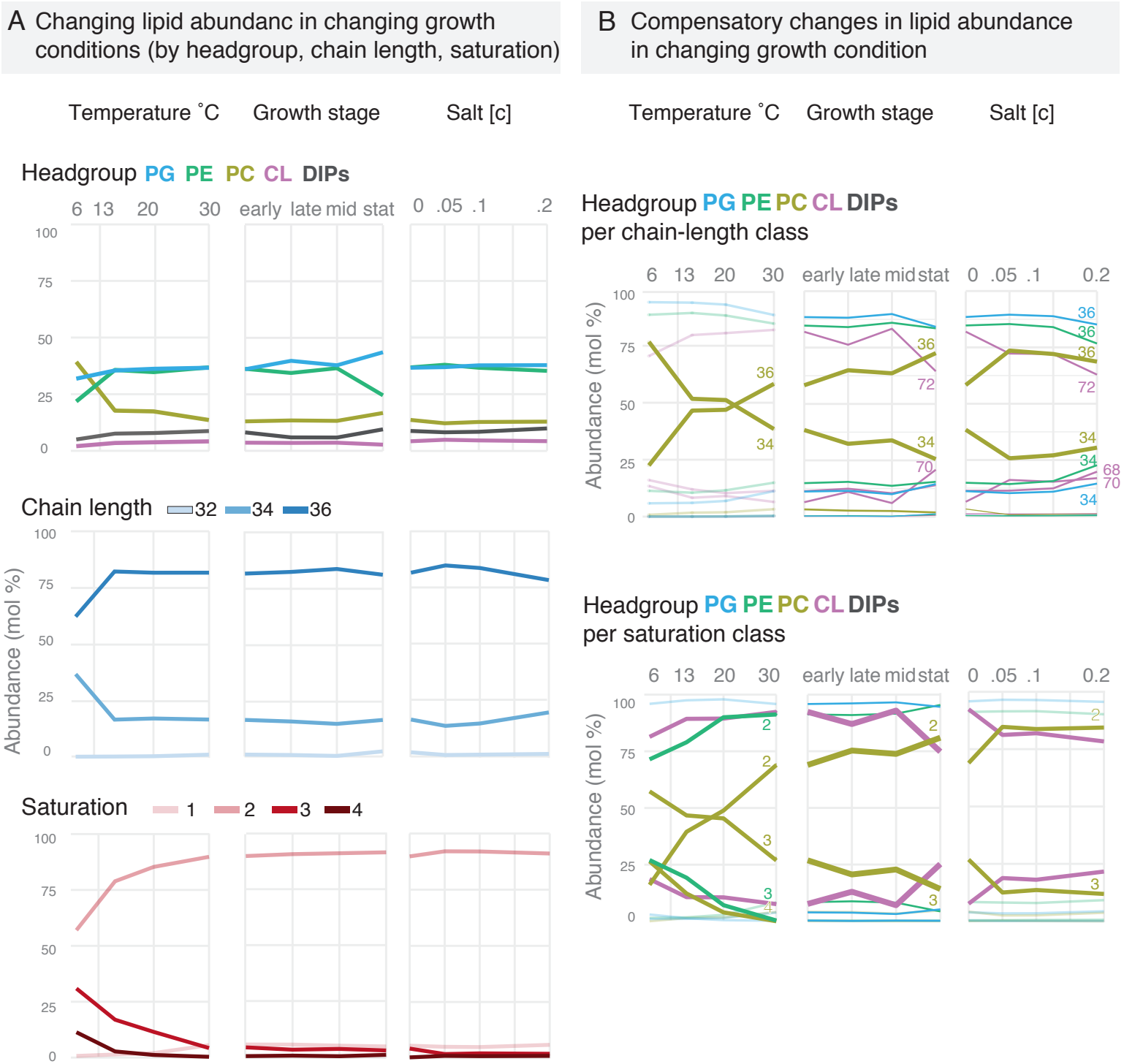

Figure 6. Step-wise adaptation of lipids by feature at changing environmental growth conditions. (A) Abundances of lipids grouped by class, acyl chain length and acyl chain saturation when changing growth temperature, probing at different growth stages, and varying salt (NaCl) concentration of the growth media. **(B)** Abundances of phospholipids grouped by acyl chain features, with headgroups indicated by color (blue: PG, green: PE, olive: PC, magenta: CL). This reveals compensatory effects in lipid adaptability: while abundance of PC with 2 double bonds increases with increasing temperatures, PC with 3 double bonds decreases from 6 to 30 degrees. In each panel, the most variable features are highlighted in bold.

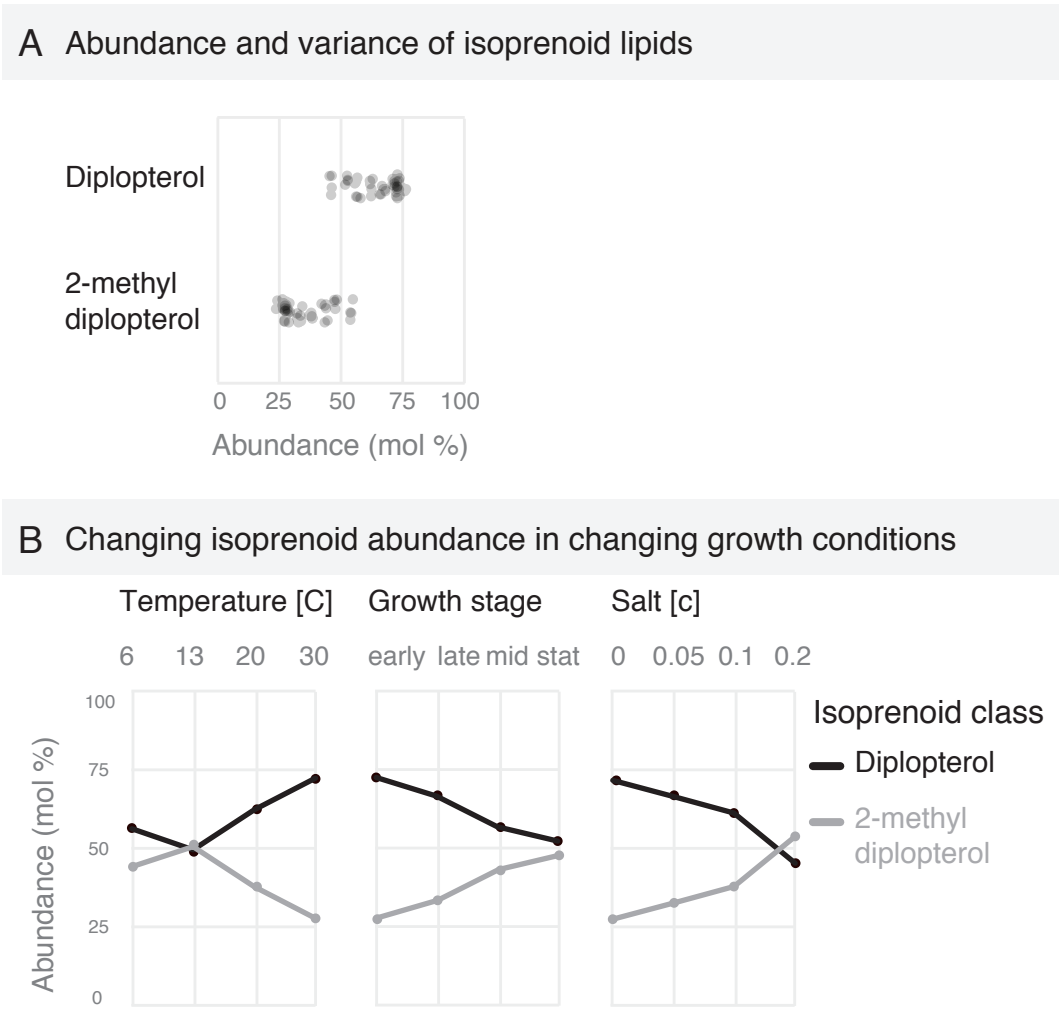

Figure 7. Diplopterol (hopanoid) methylation (A) Abundances of diplopterol species across growth conditions. **(B)** Step-wise adaptation of diplopterols when changing temperature, growth phase, and salt condition.

Methylobacterium extorquens
Gram-negative plant-based model to explore membrane adaptability

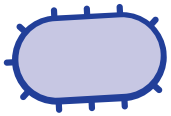

Systematic exploration of diverse enviornmental conditions
The standard growth condition (30°C, early growth phase) was adapted to new regimes.

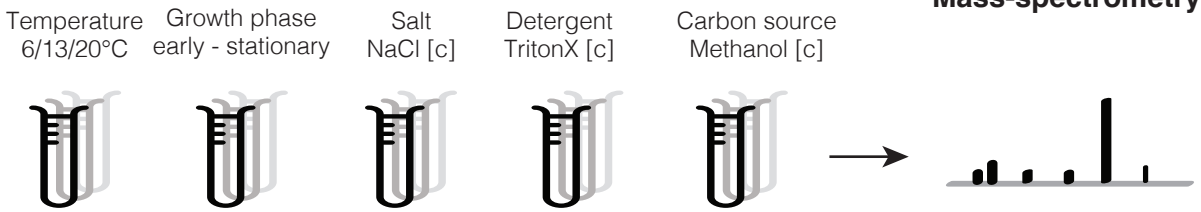

Lipids were identified and meausred by high-resolution **Quantitative Mass-spectrometry**

PCA shows robust lipidome across conditions, remodeling is notable in variable temperature conditions.

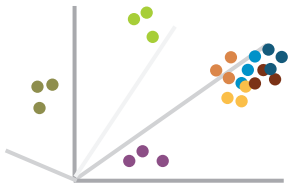

Variability across conditions: 8 lipid species were adapted in all conditions.

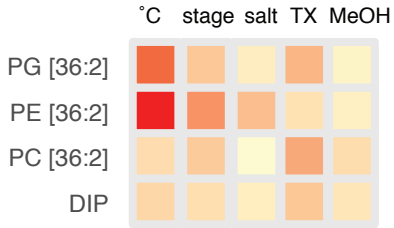

Lipidome composition assessed by lipid feature remodelling (e.g. headgroup, chain length, unsaturation) reveals complex patterns of adaptation in a simple lipidome.

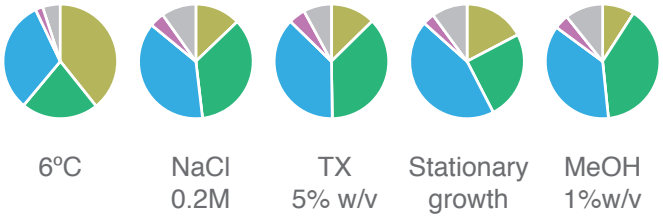

Figure 1 - supplement 1 Graphical abstract

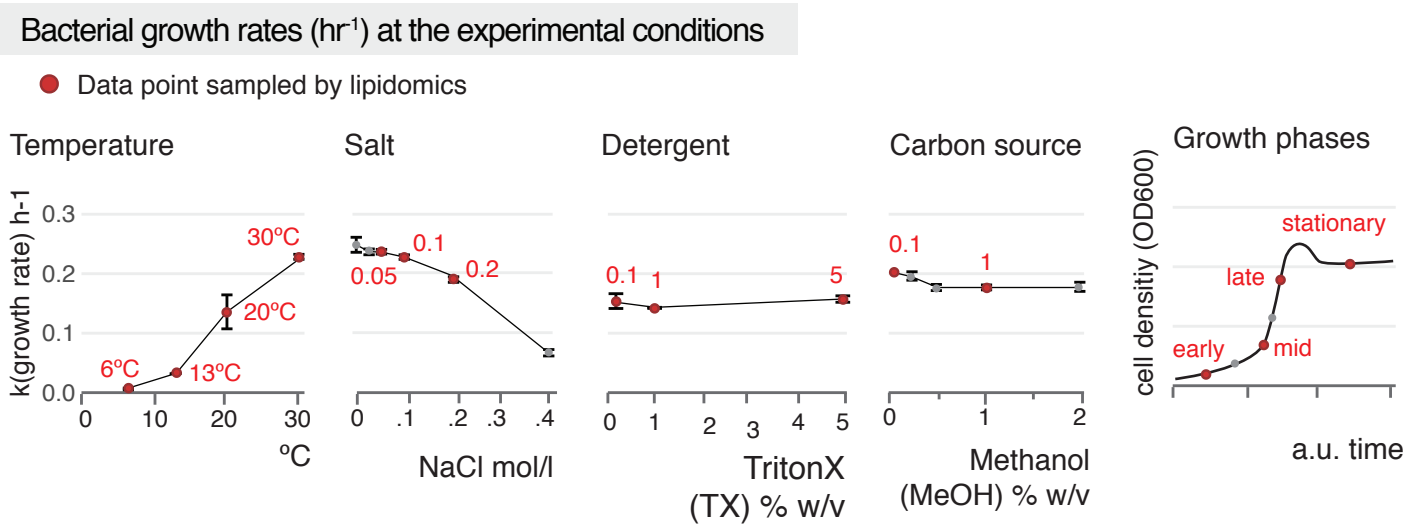

Figure 1 – Supplement 2 Bacterial growth curves and sampling points for lipidomic analysis. Chart for growth phases is a conceptual drawing.

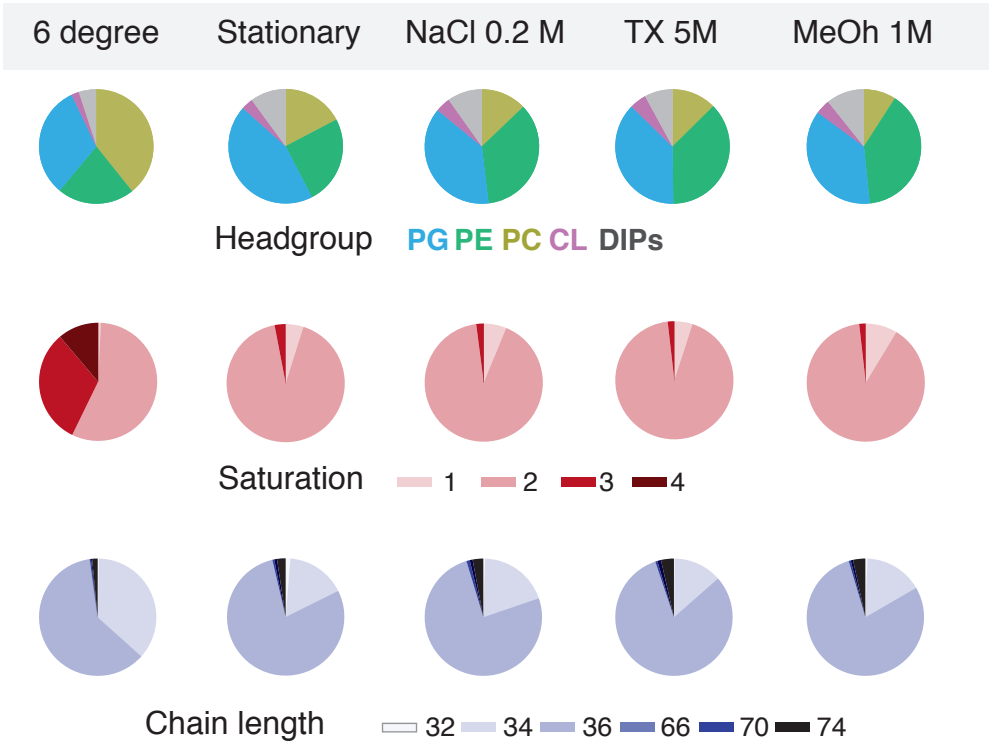

Figure 6 - Supplement 1 Overview of compositional changes across exemplary experimental conditions reveals the lipidome is robust in most growth conditions except in drastic temperature changes when the lipidome is markedly different.

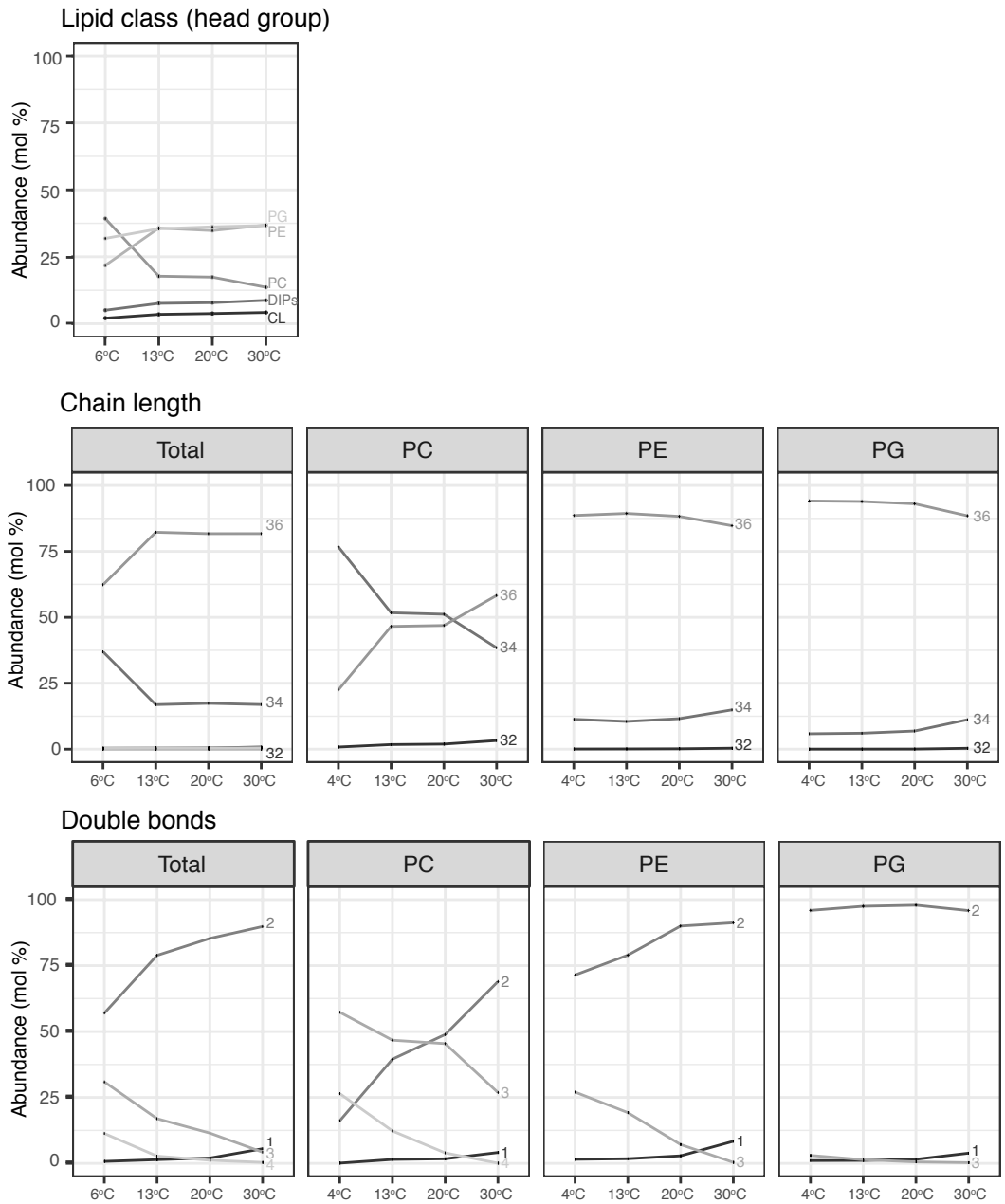

Figure 6 - Supplement 2. Step-wise adaptation of lipids by feature sampled at varying growth temperatures.

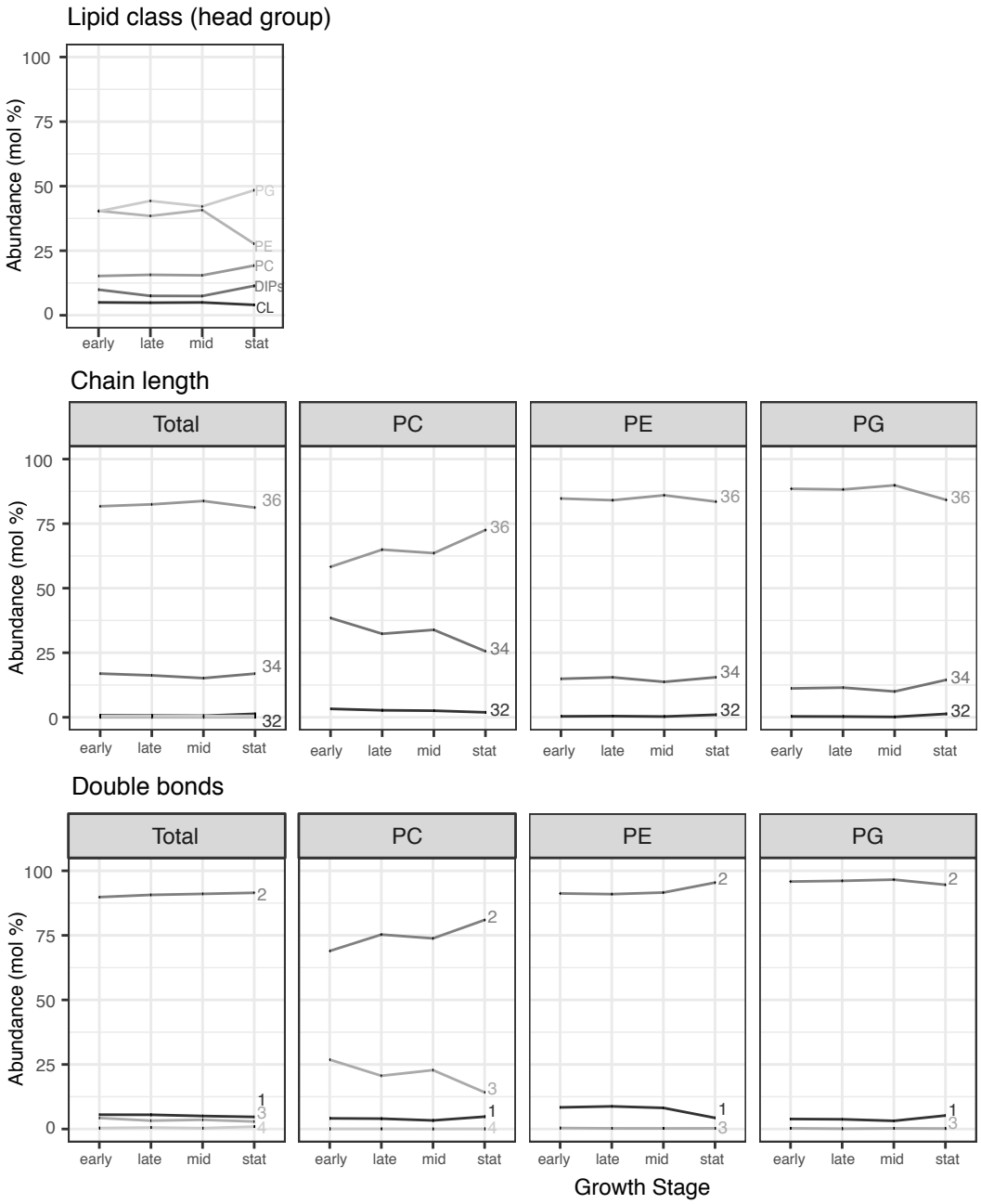

Figure 6 - Supplement 3. Step-wise adaptation of lipids by feature sampled at early, late, mid and stationary growth phase.

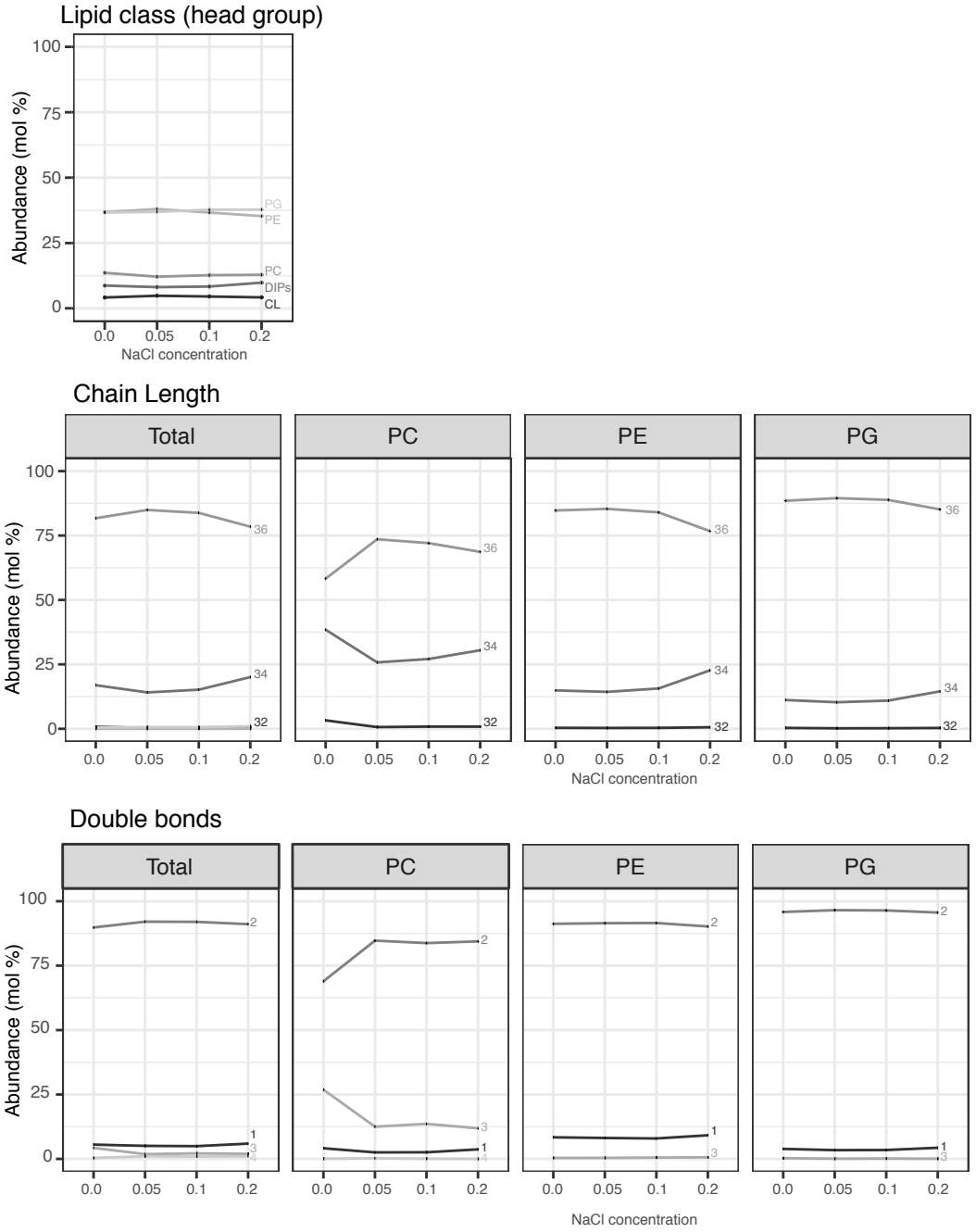

Figure 6 - Supplement 4. Step-wise adaptation of lipids by feature sampled at varying salt concentrations (NaCl).